Inorganic Chemistry

Article

pubs.acs.org/IC

Structural and Electronic Properties of Old and New $A_2[M(pin^F)_2]$ Complexes

Laleh Tahsini,[†] Sarah E. Specht,[†] June S. Lum,[†] Joshua J. M. Nelson,[†] Alexandra F. Long,[†] James A. Golen,[‡] Arnold L. Rheingold,[‡] and Linda H. Doerrer*[,†]

[†]Chemistry Department, Boston University, 590 Commonwealth Avenue, Boston, Massachusetts 02215, United States

[‡]Department of Chemistry and Biochemistry, University of California, San Diego, 9500 Gilman Drive, La Jolla, California 92093, United States

Supporting Information

ABSTRACT: Seven new homoleptic complexes of the form $A_2[M(pin^F)_2]$ have been synthesized with the dodecafluoropinacolate $(pin^F)^{2-}$ ligand, namely $(Me_4N)_2[Fe(pin^F)_2]$, **1**; $(Me_4N)_2[Co(pin^F)_2]$, **2**; $(^nBu_4N)_2[Co(pin^F)_2]$, **3**; $\{K(DME)_2\}_2[Ni(pin^F)_2]$, **4**; $(Me_4N)_2[Ni(pin^F)_2]$, **5**; $\{K(DME)_2\}_2[Cu(pin^F)_2]$, **7**; and $(Me_4N)_2[Cu(pin^F)_2]$, **8**. In addition, the previously reported complexes $K_2[Cu(pin^F)_2]$, **6**, and $K_2[Zn(pin^F)_2]$, **9**, are characterized in much greater detail in this work. These nine compounds have been characterized by UV−vis spectroscopy, cyclic voltammetry, elemental analysis, and for paramagnetic compounds, Evans method magnetic susceptibility. Single-crystal X-ray crystallographic data were obtained for all complexes except **5**. The crystallographic data show a square-planar geometry about the metal center in all Fe (**1**), Ni (**4**), and Cu (**6**, **7**, **8**) complexes independent of countercation. The Co species exhibit square-planar (**3**) or distorted square-planar geometries (**2**), and the Zn species (**9**) is tetrahedral. No evidence for solvent binding to any Cu or Zn complex was observed. Solvent binding in Ni can be tuned by the countercation, whereas in Co only strongly donating Lewis solvents bind independent of the countercation. Indirect evidence (diffuse reflectance spectra and conductivity data) suggest that **5** is not a square-planar compound, unlike **4** or the literature $K_2[Ni(pin^F)_2]$. Cyclic voltammetry studies reveal reversible redox couples for Ni(III)/Ni(II) in **5** and for Cu(III)/Cu(II) in **8** but quasi-reversible couples for the Fe(III)/Fe(II) couple in **1** and the Co(III)/Co(II) couple in **2**. Perfluorination of the pinacolate ligand results in an increase in the central C−C bond length due to steric clashes between CF_3 groups, relative to perhydropinacolate complexes. Both types of pinacolate complexes exhibit O−C−C−O torsion angles around 40°. Together, these data demonstrate that perfluorination of the pinacolate ligand makes possible highly unusual and coordinatively unsaturated high-spin metal centers with ready thermodynamic access to rare oxidation states such as Ni(III) and Cu(III).

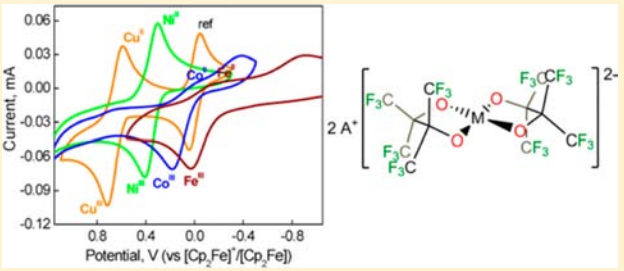

INTRODUCTION

There is a wealth of literature describing highly oxidized and reactive late transition metal complexes with N-donor ligands or mixed N,O-donor ligand systems.[1−3] Amide donor groups have been incorporated frequently into macrocyclic ligand systems of both the NR_2 variety, supporting Fe(IV)[4] and Fe(VI),[5] and the N(CO)R type[1,6] stabilizing Fe(V),[7] Co(IV),[8] Ni(III),[9,10] and Cu(III),[9,11] as well as imine donors for Co(III)[12] and mixed imine/NR_2 ligands with Ni(III).[12] These strong-donor ligand environments stabilize such higher oxidation states, and also typically engender low-spin electronic configurations. Far fewer reports exist of high-valent, late transition metal complexes in a weaker-field, all O-donor ligand environment. For example, an ornate tris(phosphonate) donor, $[CpCo\{(P(O)(R)_2\}_3]^-$, the Kläui ligand, stabilizes Co(III) in high and low spin states.[13] Co(III) is also present in insoluble $Co_2(CO_3)_3$, but it is not stable in aqueous solution except at very low pH values. Such high-spin environments are increasingly recognized as important in catalysis, including $\{MO_x\}$ species for water oxidation with Mn^{3+} and Co^{3+}.[14,15] Anionic O-donor ligands that solubilize metal centers are most commonly organic carboxylates, aryloxide, and alkoxide ligands.

Homoleptic aryloxides and alkoxides are rare as mononuclear species because the strong Brønsted basicity of these anions gives rise to bridging ligands in polymeric structures[16] in which the metal centers are coordinatively saturated and minimally reactive. Bulkier alkoxide ligands can sterically circumvent such bridging.[16−20] Decreased bridging can also be achieved electronically with fluorinated aryloxide or alkoxide ligands, which maintain open coordination sites and substrate access to the metal center. Because fluorinated alcohols are much more acidic than hydrogenated ones, e.g., the pK_a of HOC_4F_9 (5.4) vs that of HOC_4H_9 (19),[21] the conjugate bases are less basic and form terminal M-OR linkages and monomeric complexes. These effects were demonstrated by comparison of OC_6H_5

Received: July 16, 2013
Published: November 21, 2013

   dx.doi.org/10.1021/ic401837y | Inorg. Chem. 2013, 52, 14050−14063

Scheme 1. Reductive Coupling of Hexafluoroacetone

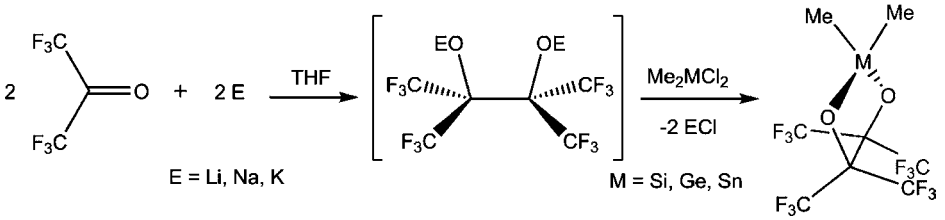

with two fluorinated aryloxide ligands, OAr^F ($Ar^F = C_6F_5$) and OAr′ (Ar′ = $C_6H_3(CF_3)_2$) in a family of late first-row transition metal complexes.[22−25] The $[M(OAr^F)_4]^{2-}$ complexes with Co(II) and Cu(II) were the first examples of homoleptic aryloxide complexes that did not require bulky ortho substitution to prevent bridged structures and were not coordinatively saturated at the metal center.[22] Use of OC_6H_5 led to the formation of dimeric structures with $[(H_5C_6O)_2M(\mu_2\text{-}OC_6H_5)_2M(OC_6H_5)_2]^{2-}$ with M = Co and Cu under the same reaction conditions used to generate the monomeric fluorinated $[M(OAr)_4]^{2-}$ complexes. Highly fluorinated aryloxides and alkoxides further endow transition metal complexes of these ligands with oxidative stability because the oxidative robustness of C−F bonds (117 kcal mol^{-1}) compared to C−H bonds (99 kcal mol^{-1})[26] diminishes unwanted ligand bond oxidation. This effect was recently demonstrated in the reactivity of Cu(I)-fluorinated alkoxides[27] with O_2 and the formation of a room-temperature stable Cu(III) diaryl compound.[28]

Herein, the electron-withdrawing power of fluorinated, O-donating groups is combined with the chelate effect in a fully fluorinated bidentate alkoxide ligand, dodecafluoropinacolate, to afford electronically and thermodynamically stabilized complexes. Perfluoropinacol is necessarily more stable toward HF elimination from its tertiary carbon than primary and secondary fluorinated alcohols in water. This ligand has been abbreviated in the literature as PFP (perfluoropinacolate),[21] ddfp (dodecafluoropinacolate),[29] and Fpin.[30] Herein and henceforth we choose to use H_2pin^F for the alcohol and $(pin^F)^{2-}$ for the deprotonated form by analogy with the extensive borate pinacolate work[31−34] that uses the abbreviation B(pin). Unlike the majority of monodentate alkoxide and aryloxide anions, which can only be used under anhydrous conditions, H_2pin^F (pK_a 5.95)[35,36] allows in situ generation of the doubly deprotonated anion by different bases under hydrous (KOH, Me_4NOH) or anhydrous ($K\{N(TMS)_2\}$) conditions to form transition metal complexes.

This potential ligand was first prepared as a lithium alkoxide intermediate formed by the bimolecular reductive coupling of hexafluoroacetone with Li shown in Scheme 1.[37] Immediate reaction of in situ generated Li-alkoxide with Me_2SiCl_2 in THF afforded the $[Me_2Si(pin^F)]$ as the first compound demonstrating bidentate chelation of the perfluoropinacolate ligand.[37] Shortly afterward, $[Na_2(pin^F)]$ was prepared by Na reduction of hexafluoroacetone in THF,[38] although no structural data were provided. The acid−base reaction of H_2pin^F and Na_3BO_3 in an aqueous solution led to the formation of $Na[B(pin^F)_2]$, the first of many compounds to be formed with this $[A(pin^F)_2]^{n-}$ stoichiometry.[39] These group 14 tetrahedral compounds, $(CH_3)_2M(pin^F)_2$ (M = Si, Ge, Sn), and $Na[B(pin^F)_2]$ are all stable under ordinary handling conditions and are resistant to acid hydrolysis, yet undergo rapid hydrolysis under basic aqueous conditions.[39]

After the initial synthesis of the ligand and its alkali metal salts, some transition metal and Al complexes were prepared and elemental analysis data provided for $[M(pin^F)_3]^{3-}$, M = Fe, Al; and $[M(pin^F)_2]^{2-}$, M = Mn, Ni, Cu, Zn.[40] In the absence of structural data, magnetic susceptibilities suggested an octahedral geometry for Fe(III) based on tri(oxalato)ferrate species, and square-planar geometries for Mn(II) and Cu(II).[40] A square-planar geometry was also suggested for the diamagnetic Ni(II) complex and this result was later confirmed by X-ray crystallography.[41] The first related Fe(II) and Co(II) complexes were recently published,[29] in which the paramagnetic complexes have the particularly unusual combination of high-spin electronic configurations and square-planar geometries whereas the diamagnetic analogue $\{K(DME)_2\}_2[Zn(pin^F)_2]$ is tetrahedral. The structures of the related cationic derivatives $PPN[Li(MeOH)_4][M(FpinH_{-2})_2]$,[42] with PPN = bis(phosphoranediyl)iminium, and M = Fe and Co have also been reported recently. Herein we expand this early work to include noncoordinating R_4N^+ cations in a thorough, comparative study that analyzes the effect of countercation and F/O atom interactions with K^+ on complex geometries. The spectroscopic properties and electrochemistry of these seven new compounds and several other known species with bidentate ligands further generalize the ability of fluorinated ligands to support high oxidation states.

EXPERIMENTAL SECTION

General Procedures. All Co(II), Cu(II), and Zn(II) complexes were prepared in air under ambient conditions. Deionized water (H_2O), EtOH, and MeOH were used as solvents for aerobic syntheses. The synthesis of **4** with Ni(II) was carried out in a N_2-filled drybox at room temperature and that of **1** with Fe(II) was conducted in a N_2-filled wet-box. All other compounds were prepared in air. The anhydrous solvents CH_2Cl_2, THF, Et_2O, and hexanes were dried in an alumina-based solvent purification system (SPS) under Ar and piped directly into a N_2-filled MBraun drybox and stored over molecular sieves. Toluene and dimethoxyethane (DME) were dried by refluxing over Na/benzophenone under an N_2 atmosphere and distilled. Acetonitrile was distilled from CaH_2 under N_2. NMR samples prepared under N_2 used d_8-THF, d_6-acetone, or CD_3CN which were stored over sieves under N_2. Celite was heated to 125 °C under vacuum overnight and stored under N_2. Potassium hydride (KH) was obtained as a mineral oil dispersion (30 wt %) and purified by washing with hexanes and drying in vacuo prior to storage in a glovebox. The alcohol H_2pin^F was obtained from Oakwood Chemicals or Matrix Scientific and was dried over sieves and distilled before use in the drybox or wet-box. All other reagents were obtained commercially and used without any further purification. UV−vis data were collected with a Shimadzu UV-3600 spectrometer, which could be equipped with a Praying Mantis diffuse reflection accessory purchased from Harrick Scientific Products Inc. Prior to measurement, all solid samples were ground to a fine powder using an agate mortar and pestle and measured against a densely packed, flat surface of finely ground $BaSO_4$. Reflectance spectra were converted to absorbance data, using the Kubelka−Munk function.[43,44] NMR spectra were measured using

dx.doi.org/10.1021/ic401837y | Inorg. Chem. 2013, 52, 14050−14063

Varian 400 and 500 MHz spectrometers. Chemical shifts (δ) for ^{1}H NMR spectra were referenced to the resonance of residual protio solvent. Solution phase magnetic susceptibilities were determined via the Evans method[45,46] in CD_3CN, d_8-THF, or d_6-acetone with $(Me_3Si)_2O$ as an internal reference and reported after appropriate diamagnetic corrections. Electron paramagnetic resonance (EPR) spectra were collected on a Bruker CW X-band ELEXSYS E 500 spectrometer equipped with an ER 4122SHQE-W1 super high sensitivity cavity, a Super-X EMB microwave source, and an ESR900 continuous flow liquid helium cryostat. Samples were prepared in 2-MeTHF with 5 mM concentration, and data collected at 9.386 Hz, 2 mW microwave power, with 5 G modulation amplitude at 4 K. Conductivity studies were performed at room temperature in the drybox using a Fisher Scientific Traceable Portable Conductivity Meter (model number 09−326−2). Elemental analyses were performed by Atlantic Microlabs, Inc. (Norcross, Georgia).

Synthetic Procedures. *$(Me_4N)_2[Fe(pin^F)_2]\cdot 2CH_3CN$, **1**·2CH$_3$CN.* A portion of $FeBr_2$ (0.324 g, 1.50 mmol) was dissolved in THF affording a deep orange solution to which 2 equiv of H_2pin^F (1.00 g, 3.01 mmol) in THF were added with stirring. After 1 h, 2 equiv of $Me_4NOH\cdot 5H_2O$ (0.544 g, 3.00 mmol) dissolved in H_2O were added dropwise over the course of 2 min, resulting in a clear brown-orange solution with a dark precipitate. After 1 h, an additional 2 equiv of $Me_4NOH\cdot 5H_2O$ (0.544 g, 3.00 mmol) in H_2O were added dropwise affording a dark blue solution with a dark precipitate. After stirring for 4 h, the solvent was removed in vacuo from the dark purple solution to yield purple and white solids. The solids were triturated once with THF, and then dissolved in acetonitrile. The cloudy purple solution was filtered through Celite and the solvent was removed in vacuo affording purple-blue solid which was recrystallized twice from a solution of acetonitrile layered with Et_2O (0.613 g, 47%). UV−vis (CH_3CN) (λ_{max}, nm (ε, M^{-1} cm^{-1})): 265 (6950), 323 (1920), 576 (18). Anal. Calcd. for $C_{20}H_{24}FeF_{24}N_2O_4$: C, 27.67; H, 2.79; F, 52.52. Found: C, 27.42; H, 2.79; F, 52.23. μ_{eff} (CD_3CN) = 5.66 μ_B.

*$(Me_4N)_2[Co(pin^F)_2]$, **2**.* A portion of $Me_4NOH\cdot 5H_2O$ (0.746 g, 3.992 mmol) was dissolved in 4 mL EtOH and then added slowly to a combined mixture of CoI_2 (0.312 g, 0.998 mmol) and H_2pin^F (0.687 g, 1.996 mmol) in 10 mL EtOH. A pink precipitate instantly formed, and the reaction mixture was stirred for 1 h at room temperature. The resulting precipitate was collected on a glass frit and dried in vacuo at which point it was transferred into a wet-box filled with N_2. Redissolving the solid in acetone afforded a red solution and white precipitate of presumed Me_4NI, which was removed via filtration. The red solution was concentrated under vacuum and then layered with Et_2O. Red needle-like crystals of X-ray quality were grown from an acetone and Et_2O mixture. The yield of triply recrystallized product was 67% (0.583 g). UV−vis (CH_3CN) (λ_{max}, nm (ε, $M^{-1}cm^{-1}$)): 233 (1552), 505 (35), 560 (57). Anal. Calcd. for $C_{20}H_{24}CoF_{24}N_2O_4$: C, 27.57; H, 2.78; F, 52.33. Found: C, 27.73; H, 2.63; F, 52.08. μ_{eff} (CD_3CN) = 4.67 μ_B.

*$(^nBu_4N)_2[Co(pin^F)_2]$, **3**.* A portion of $^nBu_4NOH$ (20 mL from 0.1 M stock solution in toluene/MeOH, 2.00 mmol) was added slowly to a combined mixture of CoI_2 (0.166 g, 0.530 mmol) and H_2pin^F (0.348 g, 1.00 mmol) in 10 mL EtOH. The resulting red-pink solution was stirred for 1 h after which time the solvent was removed in vacuo leading to viscous red oil. After extended drying under vacuum the red sticky material was brought into a wet-box and redissolved in a minimum amount of distilled THF affording a red solution and white precipitate of $^nBu_4NI$. Complete precipitation of the iodide salt was achieved by layering the THF solution with Et_2O, leaving a red solution behind. The solution was filtered again and solvent removed in vacuo. A second recrystallization of the resultant red oil in THF/hexanes afforded X-ray quality cubic red crystals. The yield of twice recrystallized product was 68% (0.435 g). UV−vis (CH_3CN) (λ_{max}, nm (ε, $M^{-1}cm^{-1}$)): 233 (1552), 505 (35), 560 (57). Anal. Calcd. for $C_{44}H_{72}CoF_{24}N_2O_4$: C, 43.75; H, 6.01; F, 37.75. Found: C, 40.62; H, 5.26 (the CH analyses are an average of two replicate runs); F, 40.45. The elemental analysis data indicate a composition with six C and H atoms removed from $(^nBu_4N)_2[Co(pin^F)_2]$ molecule. The formation of some volatile moieties like methane gas that can be swept away unburnt may account for the low C and H values observed.[47] μ_{eff} (d_8-THF) = 4.87 μ_B.

*{K(DME)$_2$}$_2$[Ni(pin^F)$_2$], **4**.* This complex was made by slight modification of the procedure for the Co and Fe analogues.[29] Under a N_2 atmosphere, a portion of NiI_2 (0.312 g, 1.00 mmol) was combined with 2 equiv of ($K\{N(TMS)_2\}$) (0.398 g, 2.00 mmol) in 14 mL of DME forming a dark green-black solution and was left to stir for 20 min. A portion of H_2pin^F (0.688 mL, 2.00 mmol) in 3 mL toluene was added and the reaction mixture was left to stir for 24 h. Addition of another 2 equiv of ($K\{N(TMS)_2\}$) (0.398 g, 2.00 mmol) in 4 mL DME made the solution dark purple and it was left to stir overnight. The reaction mixture was filtered through Celite and the dark purple filtrate concentrated to a dark brown oily solid under vacuum. The solid was triturated three times with toluene, once with DME, and once with hexanes. The product was then extracted into DME and filtered through Celite. The solution was concentrated and purple crystals were grown from a DME/hexanes mixture at −30 °C. The triply recrystallized product gave a 30% yield (0.317 g). UV−vis (THF) (λ_{max}, nm (ε, M^{-1} cm^{-1})) 395 (15), 553 (11). Anal. Calcd. for $\{K_2(DME)\}[Ni(pin^F)_2]\}$; $C_{16}H_{10}F_{24}K_2NiO_6$: C, 21.56; H, 1.13; F, 51.17. Found: C, 21.66; H, 1.01, F, 49.41. Fluorine analysis is likely low because of incomplete combustion of F atoms.

*$(Me_4N)_2[Ni(pin^F)_2]$, **5**·0.5CH$_3$CN.* A portion of H_2pin^F (0.381 g, 1.10 mmol) was mixed with a portion of $Me_4NOH\cdot 5H_2O$ (0.399 g, 2.20 mmol) in 2 mL EtOH, and was added to a solution of $Ni(NO_3)_2$ (0.160 g, 0.55 mmol) in 3 mL EtOH. The reaction mixture was then allowed to stir for 12 h after which point the solvent was removed. The resultant blue-gray solids were dissolved in acetone and filtered through a glass frit to separate a blue filtrate from a white solid, presumably KNO_3. The solvent was removed from the filtrate and the solid was redissolved in acetone and filtered again. This process was repeated five times until no further white precipitate was filtered away and only blue-purple solids remained. Vapor diffusion of Et_2O into acetonitrile at 5 °C afforded blue-purple crystals in 82% yield (0.394 g). ^{1}H NMR (CD_3CN, 400 MHz), 2.99 ppm. ^{19}F NMR (CD_3CN, 376 MHz), 56.94 ppm. UV−vis (CH_3CN) (λ_{max}, nm (ε, M^{-1} cm^{-1})): 274 (11,800), 420 (4), 546 (16), 600 (20). Anal. Calcd. for $C_{20}H_{24}F_{24}NiN_2O_4$: C, 27.58; H, 2.78; F, 52.34. Found: C, 27.42; H, 2.80; F, 51.77.

*$K_2[Cu(pin^F)_2]$, **6**·4H$_2$O.* The synthesis of this complex has been reported by Willis and co-workers,[40] however no crystal structure or spectroscopic data have been reported. In air, $Cu(NO_3)_2\cdot 3H_2O$ (0.122 g, 0.501 mmol) dissolved in 2 mL of H_2O was added to H_2pin^F (0.348 g, 1.01 mmol) dissolved in 3 mL of MeOH while stirring. Addition of an aqueous solution of KOH (0.080 g, 2.00 mmol) afforded a deep blue solution. The reaction mixture was allowed to stir for 1 h, and was then concentrated by heating at 50−60 °C. Deep blue crystals were isolated after cooling down the solution to 5 °C, and were washed further with a minimum amount of cold H_2O and dried in air with a yield of 67% (0.295 g). Blue-colored crystals suitable for X-ray analysis were grown by slow evaporation of an aqueous solution. UV−vis (CH_3CN) (λ_{max}, nm (ε, cm^{-1} M^{-1})): 195 (2960), 242 (6670), 646 (32); (H_2O) (λ_{max}, nm (ε, cm^{-1} M^{-1})): 193 (7920), 241 (6150), 668 (22). Anal. Calcd. for $C_{12}H_4CuF_{24}K_2O_6$: C, 17.12; H, 0.48; 54.16. Found: C, 16.86; H, 0.27; F, 53.09. (Fluorine analysis likely low due to incomplete combustion) μ_{eff} (CD_3CN) = 1.71 μ_B.

*{K(DME)$_2$}$_2$[Cu(pin^F)$_2$], **7**.* A solution of aqueous 4 M KOH (1.50 mL, 6.00 mmol) was added to a solution of H_2pin^F (1.005 g, 3.01 mmol) in 5 mL of MeOH. The mixture was then added to a solution of $CuSO_4\cdot 5H_2O$ (0.379 g, 1.52 mmol) in H_2O affording a deep blue solution with white precipitate (presumably K_2SO_4). The mixture was stirred for 4 h and the solvent was removed in vacuo. The pale blue powder was dissolved in MeOH and filtered to remove the remaining K_2SO_4 as a white solid. After removing the solvent, the resulting blue powder was dried under vacuum while heating (90−100 °C) for 5 h before being brought into a N_2-filled drybox for recrystallization. The crude blue solid was collected in 73% yield (0.876 g). Bright blue dichroic crystals suitable for X-ray crystallographic analysis were grown from anhydrous DME and hexanes at −34 °C. UV−vis (DME) (λ_{max}, nm (ε, cm^{-1} M^{-1})): 644 (21). Anal. Calcd. for $\{K(DME)_2\}_2[Cu-$

Table 1. Summary of X-ray Crystallographic Data Collection Parameters for $A_2[M(pin^F)_2]$ Complexes

	1·2CH_3CN	**2**	**3**	**4**	**6**·4H_2O	**7**	**8**·2CH_3CN	**9**·7H_2O
formula	$C_{24}H_{30}FeF_{24}N_4O_4$	$C_{20}H_{24}CoF_{24}N_2O_4$	$C_{44}H_{72}CoF_{24}N_2O_4$	$C_{28}H_{40}F_{24}K_2NiO_{12}$	$C_{12}H_6CuF_{24}K_2O_8$	$C_{28}H_{40}CuF_{24}K_2O_{12}$	$C_{12}H_{15}Cu_{0.50}F_{12}N_2O_2$	$C_{12}H_{14}F_{24}K_2O_{11}Zn$
M_r (g mol^{-1})	475.18	871.34	1207.97	1161.51	875.91	1166.34	479.03	933.80
T (K)	100(2)	100(2)	100(2)	173(2)	100(2)	153(2)	100(2)	150(2)
λ (Å)	0.71073	0.71073	0.71073	0.71073	0.71073	0.71073	0.71073	0.71073
cryst syst	orthorhombic	monoclinic	monoclinic	monoclinic	orthorhombic	monoclinic	orthorhombic	orthorhombic
space group	*Pbca*	*P*2/*c*	*P*2$_1$/*n*	*P*2$_1$/*n*	*Cmca*	*P*2$_1$/*n*	*Pbca*	*Pbca*
a (Å)	19.629(3)	21.2586(13)	9.5141(9)	10.9133(6)	20.380(7)	11.019(8)	19.7604(12)	11.8880(10)
b (Å)	8.4890(14)	8.2481(6)	14.5636(14)	18.0930(9)	11.210(3)	18.149(13)	8.4356(5)	11.7632(9)
c (Å)	21.115(3)	18.8198(12)	20.004(2)	11.7857(7)	10.697(3)	11.924(9)	21.1710(13)	39.823(3)
α (deg)	90	90	90	90	90	90	90	90
β (deg)	90	115.402(2)	96.4820(10)	96.890(2)	90	96.941(10)	90	90
γ (deg)	90	90	90	90	90	90	90	90
V (Å^3)	3518.5(9)	2980.9(3)	2754.0(5)	2310.3(2)	2443.7(12)	2367(3)	3529.0(4)	5568.9(8)
Z	4	4	2	2	4	2	8	8
D_x (g cm^{-3})	1.794	1.942	1.457	1.67	2.381	1.637	1.803	2.228
μ (mm^{-1})	0.594	0.760	0.433	0.748	1.460	0.782	0.784	1.393
F(000)	1904	1732	1250	1172	1700	1174	1916	3664
2θ range (deg)	2.79−26.38	2.47−26.14	1.73−26.42	2.40−26.38	2.00−28.15	2.05−25.40	2.80−25.42	3.18−26.55
no. of reflns collected	14398	21076	25573	19697	13994	32784	23961	52815
no. of unique reflns	3598	5868	5621	4711	1512	4338	3251	5768
R(int)	0.0688	0.0355	0.0331	0.024	0.0863	0.0769	0.0274	0.0446
final R indices ($I > 2\sigma$)	0.0398	0.0530	0.1001	0.0266	0.0407	0.0394	0.1036	0.0282
$R(F)^a$	0.0644	0.0675	0.1105	0.0320	0.0422	0.0504	0.1176	0.0385
R (wF^2)^b	0.0949	0.1371	0.2855	0.0670	0.1159	0.1151	0.2922	0.0667
GOF on F^2	1.006	1.102	1.034	1.070	1.152	1.043	1.081	1.045

$^aR = \Sigma||F_o| - |F_c||/\Sigma|F_o|$. $^bR(\omega F^2) = \{\Sigma[\omega(F_o^2 - F_c^2)^2]/\Sigma[\omega(F_o^2)^2]\}^{1/2}$; $\omega = 1/[\sigma^s(F_o^2) + (aP)^2 + bP]$, $P = [2F_c^2 + \max(F_o,0)]/3$.

dx.doi.org/10.1021/ic401837y | Inorg. Chem. 2013, 52, 14050−14063

Scheme 2. Old and New $A_2[M(pin^F)_2]$ complexes (M = Fe, Co, Ni, Cu, Zn)

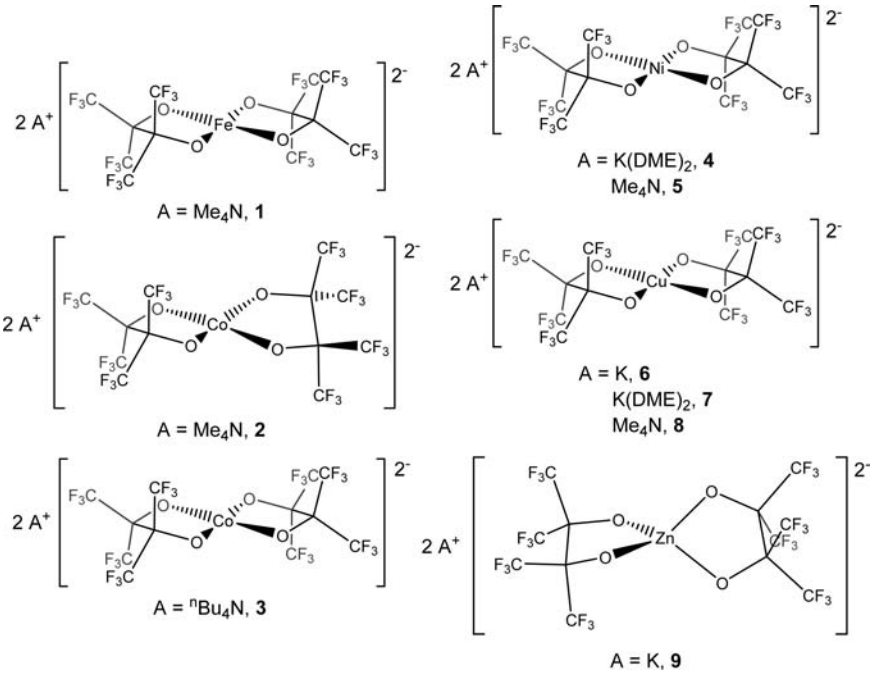

$(pin^F)_2$]; $C_{28}H_{40}CuF_{24}K_2O_{12}$: C, 28.83; H, 3.46; F, 39.09. Found: C, 27.37; H, 2.96; F, 39.65. Partial desolvation of the original sample under vacuum may account for the lower amount of C and H than the expected values, as shown with TGA in Figure S4 in the Supporting Information. μ_{eff} (d_6-acetone) = 1.93 μ_B.

*$(Me_4N)_2[Cu(pin^F)_2]\cdot 2CH_3CN$, **8**·$2CH_3CN$.* A portion of $Me_4NOH\cdot 5H_2O$ (0.561 g, 3.00 mmol) was dissolved in 4 mL EtOH along with H_2pin^F (0.517 g, 1.50 mmol) and then added to a portion of $CuBr_2$ (0.167 g, 0.75 mmol) in 6 mL EtOH. The reaction mixture was allowed to stir for 1 h after which point it was filtered through a glass frit to separate a blue filtrate from a blue-gray solid. The solvent was removed under vacuum and both solid portions were redissolved in acetone forming a blue solution with a white precipitate presumed to be Me_4NBr. Upon filtration of the precipitate and removal of the solvent in vacuo the resulting solid was redissolved in acetonitrile. Blue needlelike crystals of X-ray quality were grown by slow evaporation at room temperature. The yield of triply recrystallized product was 42% (0.304 g). UV–vis (CH_3CN) (λ_{max}, nm (ε, M^{-1} cm^{-1})): 240 (410), 570 (18), 650 (15). Anal. Calcd. for $C_{20}H_{24}CuF_{24}N_2O_4$: C, 27.42; H, 2.76; F, 52.05. Found: C, 27.15; H, 2.78; F, 51.79. μ_{eff} (CD_3CN) = 1.96 μ_B.

*$K_2[Zn(pin^F)_2]$, **9**·7 H_2O.* A portion of H_2pin^F (0.579 g, 1.68 mmol) was mixed with a solution of KOH (0.188 g, 3.36 mmol) in 2 mL of H_2O and added to a portion of ZnI_2 (0.269 g, 0.840 mmol) dissolved in 3 mL of MeOH. The resulting colorless reaction mixture was allowed to stir for 1 h at which point no precipitate had formed. The product was isolated as large colorless cubic crystals when solvent was slowly evaporated over the course of 5 days. The triply recrystallized yield was 32% (0.130 g). ^{19}F NMR (CD_3CN, 376 MHz), 70.93 ppm. UV–vis (H_2O) (λ_{max}, nm (ε, $M^{-1}cm^{-1}$)): 266 (8240); (CH_3CN): 206 (1472), 249 (1658), 273 (1368). Anal. Calcd. for $K_2[Zn(pin^F)_2]\cdot 3H_2O$; $C_{12}H_6F_{24}K_2O_7Zn$: C, 16.73; H, 0.70; F, 52.91. Found: C, 16.41; H, 0.47; F, 51.65. Fluorine analysis is likely low because of incomplete combustion of F atoms.

X-ray Crystallography. A summary of crystal data collection and refinement parameters for all compounds is given in Table 1. Crystal data for all complexes were collected on Bruker diffractometers equipped with either an APEX-CCD or CMOS detector with Mo($K\alpha$) radiation (λ = 0.71073 Å). All obtained data were corrected for absorption using the SADABS program. All structures were solved by heavy-atom methods and the remaining non-hydrogen atoms were located from subsequent difference maps. All structures were refined with anisotropic thermal parameters for all non-hydrogen atoms; hydrogen atoms were treated as idealized contributions. Hydrogen atoms associated with the water oxygen in **9** were found from a Fourier difference map and were refined isotropically with a distance of 0.84(1) Å and 1.20 U_{eq} of parent oxygen atom. All atoms of the Co anion (except Co) in **3** were disordered and were refined using a two part model. Although the anion portion of the compound exhibited extensive disorder the tetra-n-butyl ammonium portion was well behaved. Oxygen atoms O(1) and O(2) and carbon atoms C(1) and C(4) in compound **8** were treated as being disordered over two positions and were refined with EADP constraints. The high residual R value is suggestive of additional disorder but no attempt was made to address this point. The refinement of F^2 was calculated against all reflections. All esds (except the esd in the dihedral angle between two l.s. planes) are estimated using the full covariance matrix.

Electrochemistry. Cyclic voltammetry studies of **1**, **2**, **5**, and **8**, were performed in CH_3CN using a 5 mM concentration of each complex and 0.1 M of $TBAPF_6$ (tetra-n-butylammonium hexafluorophosphate) as the supporting electrolyte under an inert atmosphere using a three-electrode cell connected to an external CHI 630C potentiostat run by a personal computer with CHI software. A glassy carbon electrode (0.5 mm diameter) was employed as the working electrode, with $Ag/AgNO_3$ or Ag wire (quasi)electrode as the reference and Pt wire as the counter electrode, respectively. The working electrode was cleaned between experiments using a polishing pad and carefully dried. All voltammograms were recorded with 100 mV/s scan rate and all potentials are reported versus $[Cp_2Fe]^+/[Cp_2Fe]$ as an internal standard.

RESULTS AND DISCUSSION

Syntheses. All new $[M(pin^F)_2]^{2-}$ complexes, shown in Scheme 2, are formed by reactions of metal salts (halide, nitrate or sulfate) and H_2pin^F in the presence of a base which can be KOH, Me_4NOH,[21,40] or ($K\{N(TMS)_2\}$)[29] depending on the desired solubility, solvation, and the metal redox properties.

Reaction of a THF solution of $FeBr_2$ with H_2pin^F followed by addition of Me_4NOH in the absence of O_2 permitted the isolation of $(Me_4N)_2[Fe(pin^F)_2]$, **1**, in moderate yield. Similar addition of R_4NOH to mixtures of CoI_2 and H_2pin^F led to

dx.doi.org/10.1021/ic401837y | Inorg. Chem. 2013, 52, 14050–14063

Table 2. Selected Bond Lengths and Angles for $A_2[M(pin^F)_2]$ Complexes

complex	bond	distance (Å)	bonds	angle (deg)
1	Fe(1)−O(1)	1.9776(16)	O(1)−Fe(1)−O(2)	82.13(7)
	Fe(1)−O(2)	1.9834(17)	O(1)−Fe(1)−O(1)^{i}	180
	C(1)−C(2)	1.653(4)	O(1)−Fe(1)−O(2)^{i}	97.87(7)
2	Co(1)−O(1)	1.962(3)	O(1)−Co(1)−O(2)	84.32(12)
	Co(2)−O(4)	1.961(3)	O(1)−Co(1)−O(2)^{i}	152.50(12)
	Co(2)−O(3)	1.965(3)	O(1)−Co(1)−O(1)^{i}	101.92(17)
	O(1)−C(2)	1.364(5)	O(2)^{i}−Co(1)−O(2)	102.55(17)
	O(3)−C(8)	1.368(5)	O(4)−Co(2)−O(3)	84.60(12)
	O(4)−C(11)	1.367(5)	O(4)−Co(2)−O(3)^{ii}	151.04(12)
	C(2)−C(5)	1.652(6)	O(4)−Co(2)−O(4)^{ii}	101.97(17)
	C(8)−C(11)	1.646(6)	O(3)−Co(2)−O(3)^{ii}	103.35(17)
6	Cu(1)−O(1)	1.9053(14)	O(1)−Cu(1)−O(1)^{ii}	180.00(12)
	K(1)−O(2)	2.779(3)	O(1)−Cu(1)−O(1)^{iii}	92.79(8)
	K(1)−O(1)	2.8543(16)	O(1)−Cu(1)−O(1)^{i}	87.21(8)
	K(1)−O(3)	2.874(2)		
	K(1)−F(5)	3.0165(17)		
	C(1)−C(1)^{i}	1.631(4)		
7	Cu(1)−O(5)	1.916(2)	O(5)−Cu(1)−O(5)^{i}	180
	Cu(1)−O(6)	1.917(2)	O(5)−Cu(1)−O(6)	86.22(7)
	C(11)−C(12)	1.654(3)	O(5)−Cu(1)−O(6)^{i}	93.78(7)
	K(1)−O(5)^{i}	2.694(2)		
	K(1)−O(6)	2.688(2)		
	K(1)−O(1)	2.785(3)		
	K(1)−O(2)	2.756(2)		
	K(1)−O(3)	2.731(2)		
	K(1)−O(4)	2.811(3)		
9	Zn(1)−O(1)	1.9426(14)	O(1)−Zn(1)−O(2)	86.50(6)
	Zn(1)−O(2)	1.9634(14)	O(3)−Zn(1)−O(1)	123.43(6)
	Zn(1)−O(3)	1.9179(14)	O(1)−Zn(1)−O(4)	123.08(6)
	Zn(1)−O(4)	1.9657(14)		
	C(1)−C(4)	1.650(3)		
	C(7)−C(10)	1.657(3)		
	K(1)−O(3)	2.6977(15)		
	K(1)−O(5)	2.7694(17)		
	K(1)−O(6)	2.8442(18)		
	K(1)−O(7)	2.8257(18)		
	K(1)−O(8)	2.6707(17)		
	K(1)−F(13)	2.9268(15)		
	K(1)−F(16)	2.9831(16)		
	K(2)−O(2)	2.8650(15)		
	K(2)−O(9)	2.7308(17)		
	K(2)−O(10)	2.7412(19)		
	K(2)−F(10)	2.9916(15)		
	K(2)−F(18)	2.9291(14)		

$(Me_4N)_2[Co(pin^F)_2]$, **2**, and $(^nBu_4N)_2[Co(pin^F)_2]$, **3**, in respectable yields. The Me_4N nickel derivative, **5**, can be synthesized in a similar manner and in good yield. Two equivalents of $K\{N(TMS)_2\}$ and one of NiI_2 followed by two more equivalents of $K\{N(TMS)_2\}$ led to isolation of $\{K(DME)_2\}_2[Ni(pin^F)_2]$, **4**, presumably through intermediate $\{Ni(Hpin^F)_2\}$. No evidence is available for this intermediate, but we do not favor $\{Ni(pin^F)I]$ because our experience has shown that with a deficiency of ligand (less than two equivalents), some metal starting material is unreacted.

The Cu derivative with DME solvation can be synthesized from $CuSO_4$ with H_2pin^F in the presence of KOH to afford $\{K(H_2O)_2\}[Cu(pin^F)_2]$, **6**. Extended exposure to vacuum along with heating at 100 °C dehydrates the compound and presumably $K_2[Cu(pin^F)_2]$ forms. Recrystallizing from anhydrous DME and hexanes at −34 °C under N_2 yields $\{K(DME)_2\}_2[Cu(pin^F)_2]$, **7**. Addition of four equivalents of Me_4NOH to a mixture of $CuBr_2$ and two equivalents of H_2pin^F in wet EtOH and separation of KBr yielded the compound $(Me_4N)_2[Cu(pin^F)_2]\cdot 2CH_3CN$, **8**, which was recrystallized from acetonitrile as deep blue crystals. The reaction of ZnI_2 with two equivalents of H_2pin^F and 4 equivalents of KOH afford $K_2[Zn(pin^F)_2]\cdot 7H_2O$, **9**, in good yield in a mixture of H_2O/MeOH (2:3).

Structural Characterization. Crystallographic data collection parameters for the eight $A_2[M(pin^F)_2]$ complexes, $(Me_4N)_2[Fe(pin^F)_2]$, **1**; $(Me_4N)_2[Co(pin^F)_2]$, **2**; $(^nBu_4N)_2[Co(pin^F)_2]$, **3**; $\{K(DME)_2\}_2[Ni(pin^F)_2]$, **4**; $\{K(H_2O)_2\}_2[Cu(pin^F)_2]$, **6**; $\{K(DME)_2\}_2[Cu(pin^F)_2]$, **7**; $(Me_4N)_2[Cu(pin^F)_2]$, **8**; and $\{K(H_2O)_3\}_2[Zn(pin^F)_2]\cdot H_2O$, **9**; are summarized in

dx.doi.org/10.1021/ic401837y | Inorg. Chem. 2013, 52, 14050−14063

Table 3. Metal Coordination Environments in $[M(pin^F)_2]^{2-}$ and Selected $\{MO_4\}$ Alkoxide Complexes with M = Fe−Zn

complex ID	complex	τ_4	θ (dihedral angle, deg)	ref
GATWUV	$\{K(DME)_2\}_2[Fe(pin^F)_2]$	0	0	29
1	$(Me_4N)_2[Fe(pin^F)_2]$	0	0	this work
SEWLUD	$PPN[Li(MeOH)_4][Fe(pin^F)_2]$	0.42	46.2(11)	42
GATWOP	$\{K(DME)_2\}_2[Co(pin^F)_2]$	0	0	29
2	$(Me_4N)_2[Co(pin^F)_2]$	0.39, 0.41[a]	43.6, 41.5	this work
3	$(^nBu_4N)_2[Co(pin^F)_2]$	0	0	this work
SEWMAK	$PPN[Li(MeOH)_4][Co(pin^F)_2]$	0.51	55.6(9)	42
PUSNIB	$\{K(18C6)\}[KCo(OR^F)_4]$	0.79	89.8, 86.3	54
BIBSAG	$K_2[Ni(pin^F)_2]$	0	0	41
4	$\{K(DME)_2\}_2[Ni(pin^F)_2]$	0	0	this work
AHIPEN	$\{K(18C6)\}[KNi(OR^F)_4]$	0.74	86.8, 90.0	54
6	$K_2[Cu(pin^F)_2]$	0	0	this work
7	$\{K(DME)_2\}_2[Cu(pin^F)_2]$	0	0	this work
8	$(Me_4N)_2[Cu(pin^F)_2]$	0	0	this work
JEJCUW	$(Ph_4P)_2[Cu\{OC(CF_3)_2OH\}_4]$	0	0	52
JIWVIU	$Na_2[Cu\{OCH(CF_3)_2\}_4]$	0.23	22.5	58
HODNOD	$Ba(THF)_4[Cu\{OCH(CF_3)_2\}_4]$	0.27	25.7	51
9	$K_2[Zn(pin^F)_2]$	0.80	88.3	this work
GATXAC	$\{K(DME)_2\}_2[Zn(pin^F)_2]$	0.64	65.25	29

[a]Two crystallographically independent anions in unit cell.

Table 1. Selected distances and angles are collected in Table 2 and Table S1 in the Supporting Information for the $A_2[M(pin^F)_2]$ complexes. These homoleptic bis-(perfluoropinacolate) $A_2[M(pin^F)_2]$ complexes complement the recently reported $\{K(DME)_2\}_2[M(pin^F)_2]$ complexes,[29] and an early report of $K_2[M(pin^F)_2]$ complexes[40] that provided no structural or spectroscopic characterization, though $K_2[Ni(pin^F)_2]\cdot 4H_2O$[41] was subsequently structurally characterized.

The structures of the new $A_2[M(pin^F)_2]$ complexes are largely consistent with previously reported structures of 3*d* metals in the M(II) oxidation state, in which the A^+ cation coordinating ability (or lack thereof), and the presence of chelating ligands, play a role in observed structures. A summary of these compounds and related literature compounds with $\{MO_4\}$ coordination from fluorinated alkoxide ligands is given in Table 3, including the CSD[48] codes for published compounds. The $\{MO_4\}$ coordination geometries are quantified with τ_4 (0 = square planar, 1 = tetrahedral)[49] and the dihedral angle, θ, between the two {O−M−O} chelate rings as shown in Scheme 3.

Scheme 3. Calculation of Dihedral Angle, θ, between Two Chelating {O−M−O} Planes

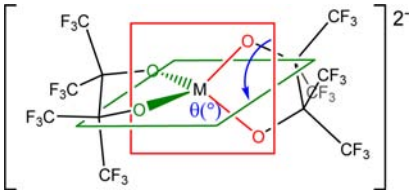

The metal coordination in $(Me_4N)_2[Fe(pin^F)_2]$, **1**, shown in Figure 1, is perfectly square-planar with four Fe−O distances averaging 1.981(17) Å. The closest contact observed between the Me_4N^+ cation and the anion oxygen atoms are the methyl H atom (calculated positions) contacts at an average distance of 2.43(3) Å. As in many of these structures, the metal atom sits on an inversion center such that there is a rigorously planar geometry about the metal center, linear trans O-M-O angles,

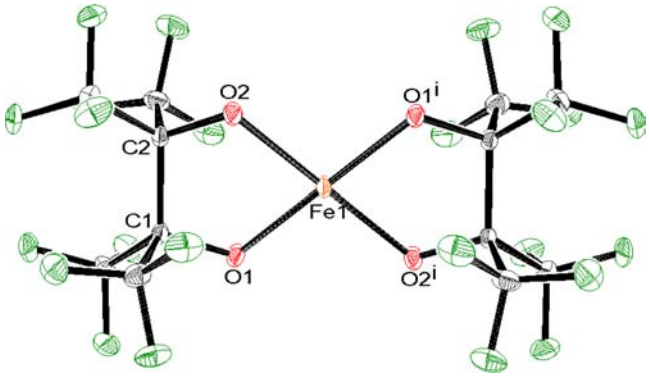

Figure 1. ORTEP diagram of the $(Me_4N)_2[Fe(pin^F)_2]\cdot 2CH_3CN$, **1**, anion. Selected distances (Å) and angles (°): Fe(1)−O(1) = 1.977(2), Fe(1)−O(2) = 1.983(2), O(1)−Fe(1)−$O(1)^i$ = 180.0, O(1)−Fe(1)−O(2) = 82.12(17), O(1)−Fe(1)−$O(2)^i$ = 97.88(7). Ellipsoids are shown at the 50% probability level.

and a dihedral angle θ of zero. In contrast, the dihedral angle in the recently reported[42] $PPN[Li(MeOH)_4][Fe(pin^F)_2]$ is 46.2(11)° due to the hydrogen-bonding network in the solid state with $(MeO)H\cdots O(pin^F)$ distances of 1.85(1) Å. The average O−Fe−O chelate angle of 82.13(7)° in **1** is slightly smaller than that in the $\{K(DME)_2\}_2[Fe(pin^F)_2]$ analog (83.34(5)°).[29]

The crystal structure of **2** is shown in Figure 2 and those of **6**, **7**, and **9** are shown in Figures 3, 4, and 5, respectively. The structures of **3**, **4**, and **8** are also shown in Figures S1− S3 in the Supporting Information. In **1**, **2**, **3**, **5**, and **8** the extensive K/H···F/O interactions observed in previously published $\{A_2[M(pin^F)_2]\}$ compounds,[29,41,42] as well as in **6** and **9**, are eliminated by replacing A^+ with R_4N^+ cations. These interactions are also decreased when K^+ is solvated with a chelating ligand, $K\{DME\}_2^+$, as in **4**, **7**, and the previously published Fe, Co, and Zn versions.[29]

The structure of $(Me_4N)_2[Co(pin^F)_2]$, **2**, has two independent molecules in the asymmetric unit, one of which is shown in Figure 2, with τ_4[49] values of 0.39 and 0.41 at the

dx.doi.org/10.1021/ic401837y | Inorg. Chem. 2013, 52, 14050−14063

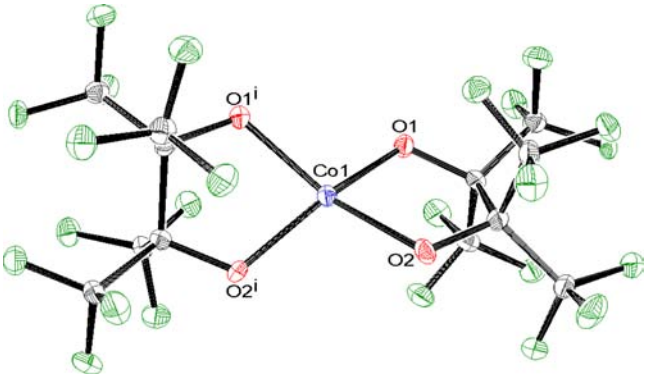

Figure 2. ORTEP diagram of the anion of $(Me_4N)_2[Co(pin^F)_2]$, **2**. Selected distances (Å) and angles (deg): Co(1)−O(1) = 1.962(3), Co(1)−O(2) = 1.962(3), O(1)−Co(1)−O(1)^i = 101.92(17), O(1)−Co(1)−O(2) = 84.32(12), O(1)−Co(1)−O(2)^i = 152.50(12). Ellipsoids are shown at the 50% probability level.

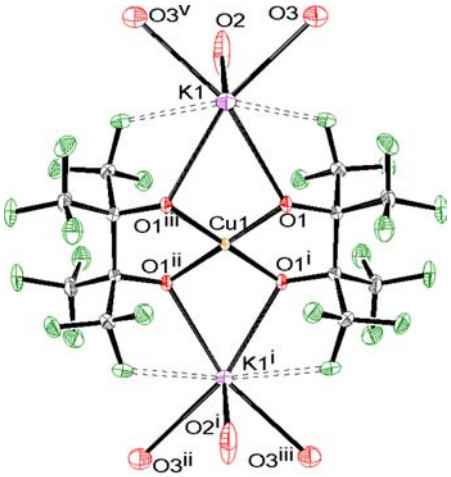

Figure 3. ORTEP diagram of $\{K(H_2O)_2\}_2[Cu(pin^F)_2]$, **6**. Selected distances (Å) and angles (deg): Cu(1)−O(1) = 1.905(14), O(1)−Cu(1)−O(1)^{ii} = 180.0, O(1)−Cu(1)−O(1)^{iii} = 92.79(8), O(1)−Cu(1)−O(1)^i = 87.21(8). Hydrogen atoms removed for clarity and ellipsoids are shown at the 50% probability level.

two Co centers, average Co−O bond distances of 1.962(3) and 1.963(3) (Å) and trans O−Co−O angles of 151.03(12) and 152.50(12)°. The average O−Co−O chelate angles of 84.32(12) and 84.60(12)° are effectively the same as 84.30(4)° as observed in $\{K(DME)_2\}_2[Co(pin^F)_2]$.[29] The average methyl H to O distance is 2.56(16) Å and the closest interionic distances to Co are 3.6062(8) from Co(1) to H(20B) and 3.5520(7) (Å) from Co(2) to H(14B). The dihedral angles of 43.6 and 41.5° for the $Co(O_{pinF})_1$/$Co(O_{pinF})_2$ planes are smaller than that in the recently reported $PPN[Li(MeOH)_4][Co(pin^F)_2]$ complex (θ = 55.6(9)°)[42] which, like the Fe analog, exhibits hydrogen-bonding between the hydroxyl groups in $\{Li(MeOH)_4\}^+$ and O atoms of pin^F at 1.845(15) Å. Figure S1 in the Supporting Information shows the structure of $(^nBu_4N)_2[Co(pin^F)_2]$, **3**, which is square planar at Co and has no close contacts between the anion and the long chain butyl ammonium cation. The average Co−O bond distance of 1.959(8) Å is slightly shorter than that in **2**. The Co atom perfectly fits at the center of inversion of the rigid $\{O_4\}$ plane. The average O−Co−O chelate angle of 77.5(3)° is smaller than the same angle in its analogous compounds

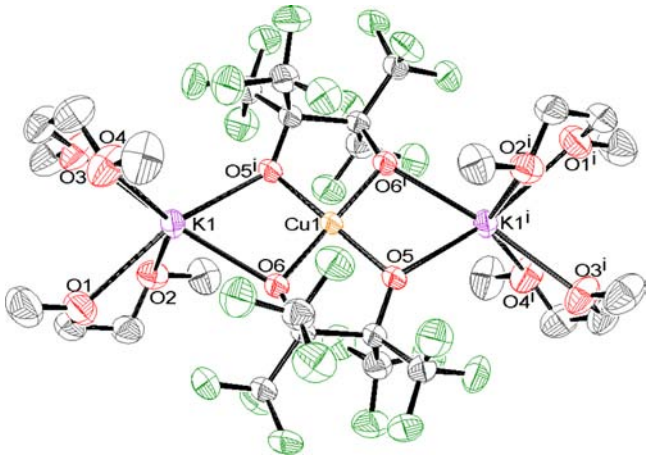

Figure 4. ORTEP diagram of $\{K(DME)_2\}_2[Cu(pin^F)_2]$, **7**. Selected distances (Å) and angles (deg): Cu(1)−O(5) = 1.916(2), Cu(1)−O(6) = 1.917(2), O(5)−Cu(1)−O(5)^i = 180.0, O(5)−Cu(1)−O(6) = 86.22(7), O(5)−Cu(1)−O(6)^i = 93.78(7). Hydrogen atoms have been omitted for clarity. Ellipsoids are shown at the 50% probability level.

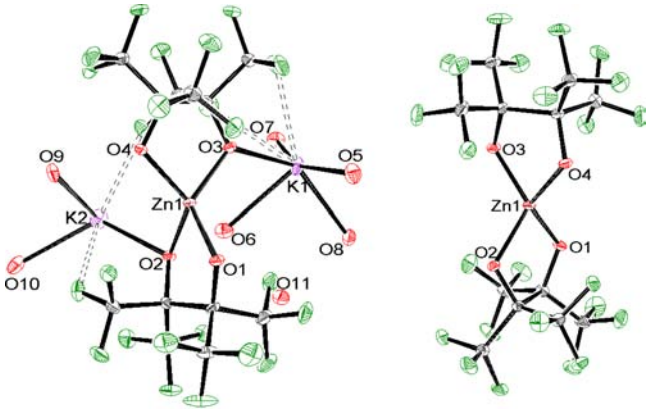

Figure 5. ORTEP diagrams of $K_2[Zn(pin^F)_2]\cdot 7H_2O$, **9** (left), and anion alone (right). Selected distances (Å) and angles (deg): Zn(1)−O(1) = 1.943(14), Zn(1)−O(2) = 1.963(14), Zn(1)−O(3) = 1.918(14), Zn(1)−O(4) = 1.966(14), O(1)−Zn(1)−O(2) = 86.50(6), O(1)−Zn(1)−O(3) = 123.43(6), O(1)−Zn(1)−O(4) = 123.08(6). For clarity, the K···O/F interactions are not shown. Ellipsoids are shown at the 50% probability level.

$(Me_4N)_2[Co(pin^F)_2]$, **2**, and $\{K(DME)_2\}_2[Co(pin^F)_2]$.[29] This fact and the anion disorder suggests that the observed structure of **3** is an average of two structures similar to that of **2** with oppositely twisted dihedral angles.

Single-crystal X-ray diffraction studies again revealed a square-planar geometry with the metal on an inversion center in the anion of $\{K(DME)_2\}_2[Ni(pin^F)_2]$, **4**, shown in Figure S2 in the Supporting Information, as was observed in the hydrated form of $K_2[Ni(pin^F)_2]$.[41] The average Ni−O bond distance (Å) in **4** is 1.858(9) and the average of K^+ interactions with O atoms on the anion is 2.674(10), which are very similar to the respective distances in $K_2[Ni(pin^F)_2]$ of 1.8527(1) and 2.8591(2).[41] Because of DME binding of K^+, there are only two K···F interactions in **4** at an average distance (Å) of 3.216(13), whereas $K_2[Ni(pin^F)_2]$ has six averaging 3.4(3). These distances in **4** are shorter than the Cu−O and K−O(pin^F) distances in the isostructural **7** described below. The average O−Ni−O chelate angle of 87.25(4)° is slightly larger

dx.doi.org/10.1021/ic401837y | Inorg. Chem. 2013, 52, 14050−14063

Scheme 4. Calculation of O−C−C−O Torsion Angle, δ, in Chelated Pinacolate Ligands

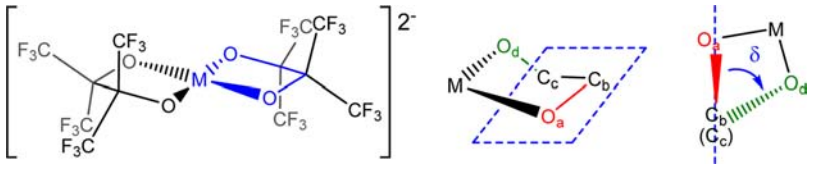

than the similar angle in **7**, whereas the angle bridged by the K^+ ion is 92.75(4)°, which is smaller than that in **7**. A tetrahedral $\{NiO_4\}$ geometry was observed in $\{K(18C6)\}[KNi(OC_4F_9)_4]$, which contains only monodentate perfluorinated t-butoxide ligands.[24] Extensive efforts have not produced a publishable crystal structure of **5**.

The Cu atoms in both **6** and **7** lie on a center of inversion and exhibit square-planar geometry with a crystallographically imposed τ_4 value[49] of 0. Compound **7** is isomorphous with the Ni analog **4**. The average Cu−O bond length is 1.905(14) Å in **6** and 1.916(2) Å in **7** with a unique K^+−O(pin^F) distance of 2.854(16) Å in **6** and 2.691(2) Å in **7**. Bridging K···F interactions are also present in **6** such that each K^+ cation has an $\{F_2O_5\}$ coordination sphere (Figure 3). The average O−Cu−O chelate angle is 87.21(8)° in **6** and 86.23(7)° in **7**, and the O−Cu−O angle bridged by K^+ ions is 92.79(8)° in **6** and 93.77(7)° in **7**. The closest intermolecular contact to Cu (not shown) is 3.277(7) Å from Cu to H(2A) in **6** and 5.380(3) Å from Cu to H(1B) in **7**, clearly demonstrating the four-coordinate nature of Cu in both complexes.

The solid-state structure of square-planar $(Me_4N)_2[Cu(pin^F)_2]$, **8**, shown in Figure S3 in the Supporting Information and isomorphous with that of **1**, shows no close contacts between cations and anions. Similar to **1** and **2**, the closest cation to anion distances are between the methyl H and pin^F O atoms at 2.42(4) Å. Similar to **6** and **7**, the Cu atom lies on a center of inversion with an average Cu−O bond length of 1.915(6) Å, and an average O−Cu−O angle of 86.1(2)°. This angle is only slightly smaller than that in **6** or **7**, demonstrating the minimal perturbation at the metal center by the bridging K^+ cations.

Three related homoleptic four-coordinate complexes of Cu(II) with monodentate fluorinated alkoxide ligands have been crystallographically characterized in $Na_2[Cu(OCH(CF_3)_2)_4]$,[50] $Ba(THF)_4[Cu(OCH(CF_3)_2)_4]$,[51] and in $(Ph_4P)_2[Cu(OC(CF_3)_2OH)_4]$.[52] The Cu−O bond lengths of **6**, **7**, and **8** are quite similar to the reported Cu−O bond lengths in the nonchelated species. The Cu centers in all three chelate complexes and the $(Ph_4P)^+$ derivative have perfectly square-planar geometry, whereas the Na- and Ba-containing compounds deviate from an ideal square-planar with τ_4 values of 0.23 and 0.27, respectively. The interaction of the Na^+ cation with the O atoms and CF_3 groups on the ligand results in a distorted geometry around the Cu(II) center in $Na_2[Cu(OCHMe^F_2)_4]$. In the structure of $(Ph_4P)_2[Cu(OC(Me^F)_2OH)_4]$, four intramolecular hydrogen bonds exist between the alkoxide O atoms and the protonated OH groups of the four gem-diolate ligands but do not distort the square-planar geometry typical for sterically unconstrained Cu(II) complexes.[53]

The ORTEP diagram in Figure 5 shows the interactions between K^+ cations and the anion of **9**. The average Zn−O(pin^F) bond distance of 1.947(14) Å is longer than the Cu−O and Ni−O distances in **7** and **5**, consistent with Zn atom's greater size. There are two nonequivalent K^+ ions in the structure, one in a $\{F_3O_5\}$ coordination environment with three K···F (average 2.955(15) Å) and five K···O (average 2.762(17) Å) interactions and the other in a $\{F_4O_4\}$ environment having four K···F (average 2.902(14) Å) and five K···O (average 2.823(17) Å) interactions with O/F atoms on the $(pin^F)^{2-}$ ligands. The average O−Zn−O angle subtended by the pin^F ligand is 86.86(6)° and the F−K−O six-membered chelate ring angles are 57.87(4) and 53.29(4)°, resulting in a τ_4 value of 0.80.

In solution, the diamagnetic **5** and **9** show only one ^{19}F resonance, suggesting that two conformations of the chelate ring may interconvert rapidly such that the C atoms bonded to O are alternately up and down with respect to the {OMO} plane. Such behavior is also consistent with the structural disorder observed in **3**, as described above.

The seven $[M(pin^F)_2]^{2-}$ structures studied to date for M = Fe (three examples) and Co (four) show that both metals can be found in either a square-planar or distorted tetrahedral geometry, depending on the cations present, as summarized in Table 3. In the absence of pin^F chelation, a tetrahedral geometry is observed in the related perfluoroalkoxide species[54] $\{K(18C6)\}[KCo(OC_4F_9)_4]$. The energetic differences are clearly small minima on a shallow potential energy surface. In contrast, six structures for Ni (three) and Cu (three) all display square planar geometries, regardless of cation, and the two known structures for Zn are close to tetrahedral. The monodentate Ni alkoxide analog $\{K(18C6)\}[KNi(OC_4F_9)_4]$ is tetrahedral,[24] whereas all known $\{CuO_4\}$ species with fluorinated nonbridging O-donor ligands are square planar.[22,55]

Compounds **6** and **9**, shown in Figures 3 and 5 respectively exhibit the shortest K···F interactions among these new structures, collected in Table S3 in the Supporting Information, which are increasingly observed when no other Lewis bases are available to the K^+ ions.[56] A bond valence analysis[57] (see Table S3 in the Supporting Information) of these two structures and five others with two equivalents of DME bound to each K clearly shows a marked decrease in the percentage of F contributions to the K coordination sphere when DME is present. The importance of these secondary K···F/O interactions in assembling two or three $\{Cu(OR)_2\}^-$ units in solution and subsequent O_2 activation has been recently reported.[27]

An interesting, but heretofore undiscussed, feature of $[M(pin^F)_2]^{2-}$ complexes is the unusually long central C−C bond length in the pin^F ligand which is almost always longer than the typical C−C length of 1.54 Å. Metal chelation of any pinacolate, fluorinated or not, favors a somewhat eclipsed configuration of the two pairs of gem-dimethyl groups, but such an orientation is opposed by steric repulsion of the methyl groups on adjacent carbon atoms. Because CF_3 groups are bulkier than CH_3 groups, more steric repulsion should be present in the fluorinated system. Greater distance between adjacent methyl groups, and therefore relief of this strain, could be achieved by lengthening the C−C bond and/or increasing the O−C−C−O torsion angles, defined in Scheme 4, in the

dx.doi.org/10.1021/ic401837y | Inorg. Chem. 2013, 52, 14050−14063

Table 4. C−C Bond Length and Torsion Angle in All $A_2[M(pin^F)_2]$ Complexes

complex ID	complex	C−C bond length (Å)	δ, torsion angle (deg)	ref
JERMOI	$(Hpy)[CrO(pin^F)_2]\cdot py$	1.612	34.446	59
		1.631	36.929	
JERMUO	$Li_2[(pin^F)CrO(\mu_2\text{-}O)_2OCr(pin^F)]\cdot(py)(H_2O)$	1.556	30.878	59
		1.570	36.874	
GATWUV	$\{K(DME)_2\}_2[Fe(pin^F)_2]$	1.653	38.037	29
1	$(Me_4N)_2[Fe(pin^F)_2]\cdot 2CH_3CN$	1.653(4)	37.0(2)	this work
SEWLUD	$PPN[Li(MeOH)_4][Fe(pin^F)_2]$	1.640	39.30	42
		1.648	39.35	
GATWOP	$\{K(DME)_2\}_2[Co(pin^F)_2]$	1.651	37.949	29
2	$(Me_4N)_2[Co(pin^F)_2]$	1.652(5)	38.9(4)	this work
		1.647(6)	39.3(4)	
3	$(^nBu_4N)_2[Co(pin^F)_2]$	1.54(2)	60(1)	this work
SEWMAK	$PPN[Li(MeOH)_4][Co(pin^F)_2]$	1.637	38.12	42
		1.645	40.69	
BIBSAG	$K_2[Ni(pin^F)_2]\cdot 4H_2O$	1.601	41.321	41
4	$\{K(DME)_2\}_2[Ni(pin^F)_2]$	1.620(2)	40.5(1)	this work
6	$K_2[Cu(pin^F)_2]\cdot 4H_2O$	1.631(3)	41.1(2)	this work
7	$\{K(DME)_2\}_2[Cu(pin^F)_2]$	1.655(4)	40.0(2)	this work
8	$(Me_4N)_2[Cu(pin^F)_2]2\cdot CH_3CN$	1.58(2)	38(1)	this work
9	$K_2[Zn(pin^F)_2]\cdot 7H_2O$	1.650(3)	40.3(2)	this work
		1.657(3)	39.9(2)	
GATXAC	$\{K(DME)_2\}_2[Zn(pin^F)_2]$	1.645	38.256	29
		1.588	7.051	
DACVAE	$[W(pin^F)(NH_2{}^tBu)(N{}^tBu)_2]$	1.622	36.309	60
WATPEM	$Li[W(pin^F)_2(Cl)(NPh)]\cdot(PhCH_3)(Et_2O)$	1.634	35.531	61
		1.631	38.134	

ligand backbone. These two parameters are summarized in Table 4 for all crystallographically characterized pin^F complexes. The new $[M(pin^F)_2]^{2-}$ complexes in the current study also have C−C bond lengths and ligand torsion angles in the same range (Figure 6) except for **8** and **3**. The observed disorder in

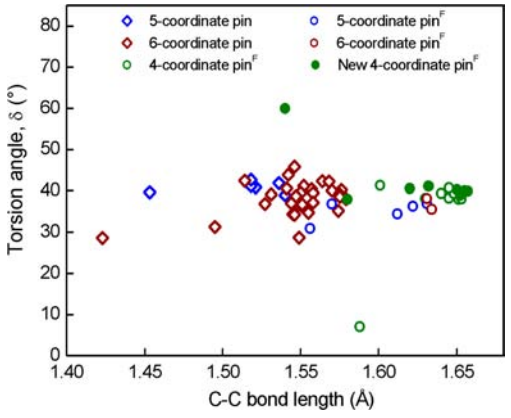

Figure 6. Central ligand C−C bond lengths (Å) and ligand torsion angles (δ, deg) in pinacolate (pin) and perfluoropinacolate (pin^F) complexes.

the O and C atoms of these anions leads to some uncertainty in the exact position of these atoms in the structure and may account for the relatively short C−C distances and large esds of 1.58(2) Å in **8** and 1.54(2) Å in **3**, which are obtained from the best models. Changing the counterion of $[Co(pin^F)_2]^{2-}$ and $[Fe(pin^F)_2]^{2-}$ complexes from K^+ to the noncoordinating Me_4N^+ did not change the C−C bond length or ligand torsion angles in either case, although it has affected the metal center geometry from purely square-planar (τ_4 = 0) in $\{K\text{-}(DME)_2\}_2[Co(pin^F)_2]$ to the distorted square-planar (τ_4 = 0.4) in $(Me_4N)_2[Co(pin^F)_2]$. These lengthend C−C bonds are not present in the crystallographically characterized compounds of nonfluorinated pinacolate, collected in Table S2 in the Supporting Information, in which the average C−C distance is 1.54(3) Å.

Within both ligand groups, however, there is no significant difference in the absolute value of the O−C−C-O torsion angles. Figure 6 shows the range of C−C bond lengths and torsion angles for all crystallographically characterized pin^F (circles) and pinacolate (diamonds) complexes to date. These data have been subdivided by coordination number as well. The increased C−C bond length is therefore the only mechanism used by these complexes for reducing the steric clash of the CF_3 groups in pin^F complexes, which is not required in non-fluorinated pinacolate derivatives. We also note that square-planar $[M(pin)_2]^{2-}$ species are unknown to date, providing further evidence of the power of these fluorinated ligands to generate low-coordinate, mononuclear complexes where non-fluorinated ligands fail.

Electronic Structure. The extensive series of $[M(pin^F)_2]^{2-}$ compounds in hand has also been analyzed by UV−vis spectroscopy and solution-based magnetic susceptibility. These studies were used to determine whether solvent binding occurs to the four-coordinate metal centers, and what affect cation choice has on solution behavior. In the Fe and Co complexes high-spin configurations were observed in all cases, and the Cu species are S = 1/2 centers. Both the Ni and Zn species are diamagnetic.

The electronic spectra of $(Me_4N)_2[M(pin^F)_2]$ where M = Fe (**1**), Co (**2**), Ni (**5**) and Cu (**8**) in CH_3CN are shown in Figure 7. All compounds reveal an intense charge transfer band in the UV range of 240−400 nm, and much weaker d−d transition

dx.doi.org/10.1021/ic401837y | Inorg. Chem. 2013, 52, 14050−14063

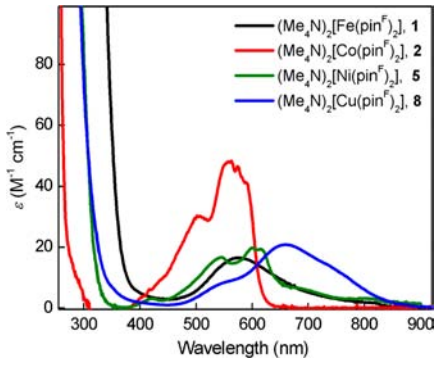

Figure 7. UV−vis spectra of $(Me_4N)_2[M(pin^F)_2]$ in CH_3CN, M = Fe, Co, Ni, and Cu.

bands between 450−750 nm. The UV−vis absorption spectrum of $(Me_4N)_2[Fe(pin^F)_2]$, **1**, in an air-free CH_3CN solution reveals a weak $d-d$ transition band at 575 nm (ε = 17 M^{-1} cm^{-1}) and very strong charge transfer band(s) at <400 nm. The exposure of this solution to air leads to the loss of chromophore at 575 nm as well as the development of a very intense absorption at <500 nm (see Figure S5 in the Supporting Information). Further details on the chemical oxidation chemistry of this system will be reported separately.

Both $(Me_4N)_2[Co(pin^F)_2]$, **2**, (Figure 7) and $(^nBu_4N)_2[Co(pin^F)_2]$, **3**, (Figure 8) in CH_3CN show three absorption bands

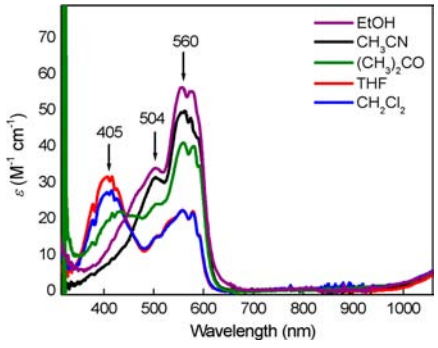

Figure 8. UV−vis spectra of $(^nBu_4N)_2[Co(pin^F)_2]$, **3**, in various solvents.

at 504 nm (ε = 31 M^{-1} cm^{-1}), 560 nm (ε = 50 M^{-1} cm^{-1}) and 574 nm (ε = 48 M^{-1} cm^{-1}). The electronic spectra of **3** exhibit solvent dependence as shown in Figure 8. The relative intensity of the absorption at 405 nm is stronger in less donating solvents, e.g., CH_2Cl_2 and THF, but stronger at 560 nm in acetone, CH_3CN, and EtOH. The same behavior was observed with $\{K(DME)_2\}_2[Co(pin^F)_2]$ analogue (see Figure S6 in the Supporting Information), which is attributed to an equilibrium between unsolvated four-coordinate and five-coordinate solvent-bound cobalt species in solution (eq 1).

$$[Co(pin^F)_2]^{2-} + L \rightleftharpoons [Co(pin^F)_2(L)]^{2-}\ L = \text{solvent} \quad (1)$$

The spectrum of $(Me_4N)_2[Ni(pin^F)_2]$, **5**, in CH_3CN (Figure 7) has three absorption bands at 545 nm (ε = 17 M^{-1} cm^{-1}), 600 nm (ε = 20 M^{-1} cm^{-1}), and 614 nm (ε = 19 M^{-1} cm^{-1}) and a less intense band at 424 nm (ε = 3.1 M^{-1} cm^{-1}), which are clearly distinct from those in acetone (see Figure S6 in the Supporting Information). The electronic spectra of $\{K(DME)_2\}_2[Ni(pin^F)_2]$, **4**, in CH_3CN, acetone, and THF have a broad absorption band with two λ_{max} at 574 nm (ε = 20 M^{-1} cm^{-1}) and 650 nm (ε = 16 M^{-1} cm^{-1}) and a much weaker band at 396 nm (ε = 9 M^{-1} cm^{-1}) (see Figure S7 in the Supporting Information), which are largely solvent independent, in contrast to those of **3** (Figure 8). Unlike the isostructural cobalt complexes, whose spectral features are independent of coordinating or noncoordinating cations, the cation and anion interaction in **4** seems to extend beyond the solid state and persist in solution. In contrast, the electronic spectra of **5**, as shown in Figure S6 in the Supporting Information, present different features with the relative intensities dependent on solvent. The absorption band at 545 nm in CH_3CN of **5** is absent from the electronic spectrum in acetone, and the broad shoulder at 450 nm is more intense in acetone. This type of spectral change as already observed with the analogous cobalt complexes (Figures 8 and S4) is again attributed to solvent binding to the metal center. The independence of the absorption spectrum of **4** from solvent polarity and/or Lewis basicity suggests that solvent binding to the $[Ni(pin^F)_2]^{2-}$ core, and concomitant increase in coordination number, requires a change in metal coordination geometry not allowed by the $\{K(DME)_2\}^+$ moieties. The $(Me_4N)^+$ salt **5** is not so hindered.

Diffuse reflectance spectra for **2**, **4**, **5**, and $K_2[Ni(pin^F)_2]$[41] are presented in Figure S10 in the Supporting Information. The electronic spectra of **2** in solution and the solid state are very similar, including the broad feature between 500 and 600 nm, demonstrating very similar coordination in solution and the solid state. The diffuse reflectance spectra of **4** and $K_2[Ni(pin^F)_2]$ are also quite similar to each other, but differ from that of **5**, supporting the hypothesis that the coordination environment in **5** is distinct from those in **4** and $K_2[Ni(pin^F)_2]$. Furthermore, Figure S11 in the Supporting Information shows the solution conductivity data in an Onsager plot for **4**, **5**, and $K_2[Ni(pin^F)_2]$, as well as the controls $\{K(18C6)\}_2[Cu(OAr^F)_4]$, $(nBu_4N)PF_6$, and Cp_2Fe in CH_3CN. Among the three Ni derivatives, there is clearly distinct behavior for **5**, namely, that it exhibits conductivity on par with that of the 2:1 electrolyte $\{K(18C6)\}_2[Cu(OAr^F)_4]$.[22] The conductivities of **4** and $K_2[Ni(pin^F)_2]$ are both slightly less than that of the 1:1 electrolyte $(nBu_4N)PF_6$, but above that of Cp_2Fe. Therefore the coordination of K^+ ions to the anion in **4** and $K_2[Ni(pin^F)_2]$, whether coordinated or prepared with H_2O or DME, persists to a large extent in solution, which cannot be the case with Me_4N^+. Altogether the solution and solid-state electronic spectra and solution conductivity data support the conclusion that the coordination environment of $[Ni(pin^F)_2]^{2-}$ moiety is different with Me_4N^+ versus K^+ cations, and by comparison to the structures of **4** and $K_2[Ni(pin^F)_2]$, which are rigidly square planar, **5** is likely to be distorted away from this geometry.

The electronic spectrum of $(Me_4N)_2[Cu(pin^F)_2]$, **8**, in CH_3CN, is shown in Figure 7 and reveals a $d-d$ transition band at 660 nm (ε = 21 M^{-1} cm^{-1}) that is blue-shifted to 646 nm (see Figure S8 in the Supporting Information) in $K_2[Cu(pin^F)_2]$, **6**, which also has an intense absorbance at ~300 nm. The electronic spectrum of a 250-times more dilute solution of **6** in CH_3CN reveals a relatively intense absorption at 275 nm (ε = 4750 M^{-1} cm^{-1}) that is absent from the spectrum of **6** in H_2O (see Figure S8 in the Supporting Information). Assuming that the K^+ ions in **6** fully dissociate in H_2O, the presence of a second band in CH_3CN solution suggests the persistence of $K^{\cdots}O/F$ interactions in solution. The similarity of the spectrum of **8**, with completely dissociated

dx.doi.org/10.1021/ic401837y | Inorg. Chem. 2013, 52, 14050−14063

cations and anions, to that of **6** in water further supports this hypothesis. The electronic spectrum of $K_2[Zn(pin^F)_2]\cdot 7H_2O$, **9**, in CH_3CN only reveals two intense charge transfer bands at 249 nm (ε = 1658 M^{-1} cm^{-1}) and 273 nm (ε = 1368 M^{-1} cm^{-1}) as is expected for a d^{10} metal center (see Figure S9 in the Supporting Information).

The EPR data for $\{K(DME)_2\}_2[Cu(pin^F)_2]$, **7**, are well-resolved and shown in Figure S12 in the Supporting Information, which reveal an anisotropic spectrum with $g_\parallel$ = 2.26 and $g_\perp$ = 2.04, and hyperfine values from the Cu nucleus of $A_\parallel$ = 0.0167 and $A_\perp$ = 0.00295 cm^{-1}, respectively. A related Cu(II) $\{CuO_n\}$ system is that of tetragonally distorted $[Cu(OH_2)_6]^{2+}$, which was reported[62] in 60% glycerine at −20 °C to have $g_\parallel$ = 2.400 and $g_\perp$ = 2.099, and hyperfine values of $A_\parallel$ = 0.01278 and $A_\perp$ = 0.00126 cm^{-1}.

Electrochemistry. The results obtained are summarized in Table 5. As shown in Figure 9 and Table 5, the cyclic voltammogram of **8** shows a reversible Cu(III)/Cu(II) couple with $E_{1/2}$ at 0.654 V (vs $[Cp_2Fe]^+/[Cp_2Fe]$). The reversible Ni(III)/Ni(II) couple of **5** appears at a lower potential than that of **8**, namely 0.356 V (vs $[Cp_2Fe]^+/[Cp_2Fe]$). A reversible peak was absent in the cyclic voltammogram of **2** (Figure 9), but the estimated $E_{1/2}$ of Co(III)/Co(II) was even further shifted to lower potentials at 0.094 V (vs $[Cp_2Fe]/[Cp_2Fe]^+$). The presence of another reduction feature at −0.378 V (vs $[Cp_2Fe]/[Cp_2Fe]^+$) is consistent with a geometric and/or electronic rearrangement in this process. The estimated $E_{1/2}$ potential of the Fe(III)/Fe(II) couple from **1** is even lower than the Co(III)/Co(II) couple of **2**. Although the reduction peak of this species was much less intense than oxidation feature, its large separation from the subsequent reduction event at −0.907 V (vs $[Cp_2Fe]^+/[Cp_2Fe]$) makes the calculated $E_{1/2}$ of −0.060 V (vs $[Cp_2Fe]^+/[Cp_2Fe]$) a reasonable value for the Fe(III)/Fe(II) redox couple of **1**. No other reduction process was observed within the solvent limit for any of these four complexes. The observed increase in the M(III)/M(II) oxidation potential of $[M(pin^F)_2]^{2-}$ complexes from Fe to Cu is consistent with increased effective nuclear charge from left to right in the periodic table. Complexes **8** and **5** can be positioned below strong oxidants such as $[Fe(bipy)_3]^{3+}$ and $[Fe(\eta_5\text{-}C_5H_4COMe)_2]^+$ with the oxidation potentials fitting in the range of 0.35−0.65 V (vs $[Cp_2Fe]^+/[Cp_2Fe]$).[63] Reversible Cu(III)/Cu(II) and Ni(III)/Ni(II) potentials have also been demonstrated in a series of dozens of complexes with oligopeptide ligands.[64−66] Two particular examples are chosen for comparison here, that of the $[M(Aib_3)]^{0/1-}$ compounds in which (Aib_3) is the fully (triply) deprotonated form of the tripeptide of aminoisobutyric acid, H_3Aib_3.[9] In these two complexes, the Ni(III)/Ni(II) couple is higher at 0.84 V (vs NHE) than the related Cu one at 0.66 V (vs NHE). Other tetradentate ligands with amide donors stabilize high oxidation states at low potentials including a peralkylated tetraamide macrocycle[10] with Ni(III)/Ni(II) at the weakly oxidizing −0.58 V (vs $[Cp_2Fe]^+/[Cp_2Fe]$) and a mixed diamide/diaryl(alk)-oxide ligand family with Cu(III)/Cu(II) couples[11] in the range ~0.14 to −1.08 V (vs $[Cp_2Fe]^+/[Cp_2Fe]$). The moderate-donor pin^F ligand clearly demonstrates that ligand fluorination can also stabilize high oxidation states, similar to the strongly donating amide groups from tripeptides, although not at as high potentials.

Interestingly, no Ni(III)/Ni(II) redox couple was observed for **4** within the solvent anodic potential limit in either CH_3CN or DME. This unusual inertness corresponds to a lack of solvent binding by **4** under conditions in which **5** takes a fifth ligand. Other ligand systems have demonstrated that formation of Ni(III) is favored for higher coordination numbers. Solvent-dependent electrochemistry of a variety of Ni complexes with hexaaza macrocycles,[67] arsine[68] and Schiff-base[69] ligands has been observed in which oxidation of Ni(II) to Ni(III) takes place at lower potentials or has a smaller peak-to-peak separation in donor solvents than nondonor or weakly coordinating solvents. The K···F/O interactions observed in the solid state for **4** may persist either totally or partially in solution and electronically prohibit solvent binding to the Ni metal center, whereas the noncoordinating nature of Me_4N^+ ions in **5** may facilitate deviation from square-planar geometry and the formation of a solvated Ni(III) species.

Table 5. Cyclic Voltammetry Data for 1, 2, 5, 8, and Comparison to Literature Complexes

complex		$E_{1/2}^{ox}$ (V)[a]	ΔE_p (V) = $E_{pa} - E_{pc}$	ref
	$[Ru(phen)_3]^{2+}$	0.87		63
	$[Fe(bipy)_3]^{2+}$	0.66		63
8	$(Me_4N)_2[Cu(pin^F)_2]$	0.654	0.128	this work
	$[Ni(Aib)_3]$	0.44[b]		9
5	$(Me_4N)_2[Ni(pin^F)_2]$	0.356	0.108	this work
	$[Cu(Aib)_3]$	0.26[b]		9
2	$(Me_4N)_2[Co(pin^F)_2]$	0.094	0.176	this work
	$[Cu\{(N(CO)R)_2(OAr)_2\}]^{2-}$	0.025		11
1	$(Me_4N)_2[Fe(pin^F)_2]$	−0.060	0.178	this work
	$[Ni\{(N(CO)R)_4\}]^-$	−0.58[c]		10
	$[Cu\{(N(CO)R)_2(OR)_2\}]^{2-}$	−1.080[d]		11

[a]Recorded vs $[Cp_2Fe]^+/[Cp_2Fe]$ in CH_3CN containing 5 mM $(Me_4N)_2[M(pin^F)_2]$ complexes, $E_{1/2} = (E_{pa} + E_{pc})/2$, where E_{pa} and E_{pc} are anodic and cathodic peak potentials, respectively. [b]Recorded in aqueous solution vs NHE and converted to $[Cp_2Fe]^+/[Cp_2Fe]$ scale by subtracting 0.4 V. [c]Recorded vs $[Cp_2Fe]^+/[Cp_2Fe]$ in CH_2Cl_2 with 0.1 M $TBAClO_4$ as supporting electrolyte. [d]Recorded vs $[Cp_2Fe]^+/[Cp_2Fe]$ in CH_3CN with 0.1 M $TBAPF_6$ as supporting electrolyte.

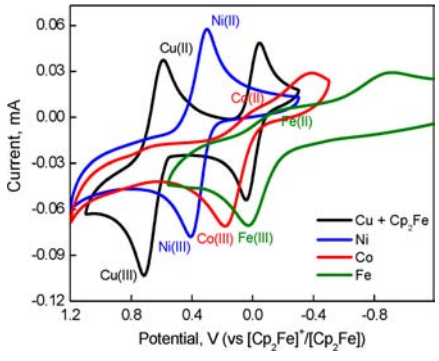

Figure 9. Cyclic voltammograms of $(Me_4N)_2[M(pin^F)_2]$, M = Fe (**1**), Co (**2**), Ni (**5**), and Cu (**8**) vs $[Cp_2Fe]^+/[Cp_2Fe]$ in CH_3CN at a scan rate of 100 mV s^{-1}.

dx.doi.org/10.1021/ic401837y | Inorg. Chem. 2013, 52, 14050−14063

CONCLUSION

The syntheses of seven new homoleptic late 3d transition metal complexes with the bidentate perfluoropinacolate (pin^F) ligand are reported herein with full structural, spectroscopic, magnetic, and electrochemical characterization. Together with previous work, a large family of these compounds now demonstrates the generality of using fluorinated O-donor ligands to generate coordinatively unsaturated, high-spin late 3d transition metal complexes. All divalent Ni and Cu species are square-planar, all Zn compounds are tetrahedral, and the geometry of Fe and Co complexes can be affected by the countercation. Cation-based effects are also observed in the electronic spectra of $\{K(DME)_2\}_2[Ni(pin^F)_2]$, **4**, and $(Me_4N)_2[Ni(pin^F)_2]$, **5**, in which the latter coordinates solvent, but not the former. Regardless of cation, the $[Co(pin^F)_2]^{2-}$ complexes bind strongly donating solvents.

All structurally characterized pin^F complexes have considerably elongated C−C bonds which are the result of steric pressure between CF_3 groups on adjacent carbon atoms. In the Ni compounds, no oxidation is observed with the $K(DME)_2^+$ cations in **4**, consistent with need for a geometry change upon oxidation that is observed in **5**. Reversible M(III)/M(II) redox couples with M = Ni and Cu and quasi-reversible couples with Fe and Co demonstrate that the fluorinated, all O-donor environment also stabilizes high oxidation states. Thus the bidentate fluorinated pinacolate ligand demonstrates the generality of low coordination number and high spin states that had been observed with monodentate aryloxides and alkoxides. In addition, the postulated unusually high oxidation states have now been achieved for the first time in these all O-donor systems.

ASSOCIATED CONTENT

Supporting Information

X-ray crystallographic data for compounds **1**−**4**, and **6**−**9** in CIF format, ORTEP diagrams and selected bond distance and angle data for **3**, **4**, and **8**, TGA data and EPR spectrum for **7**, electronic spectra of **1** in CH_3CN after air exposure, $\{K(DME)_2\}_2[Co(pin^F)_2]$ and **4** in different solvents, **5** in CH_3CN and acetone, **6** and **8** in CH_3CN and H_2O in low and high concentration, and **9** in CH_3CN, diffuse reflectance spectra and Onsager plot for {Ni(pinF)} species, table of pinacolate ligand C−C bond distances and torsion angles and a tabulated K···F bond valence analysis for **6** and **9** and all known $\{K(DME)_2\}_2[M(pin^F)_2]$ complexes. This material is available free of charge via the Internet at http://pubs.acs.org.

AUTHOR INFORMATION

Corresponding Author

*E-mail: doerrer@bu.edu. Phone: +1 (617) 358 4335. Fax: +1 (617) 353 6466.

Notes

The authors declare no competing financial interest.

ACKNOWLEDGMENTS

We thank Boston University, NSF-CHE 0619339 (NMR spectrometer in the Chemical Instrumentation Center at Boston University), NSF-CRIF 0840418 (EPR Spectrometer in the BU Chemical Instrumentation Center), and DOE-BES DE-FG02-11ER16253 (LHD) for financial support.

REFERENCES

(1) Collins, T. J. *Acc. Chem. Res.* **1994**, *27*, 279.
(2) Boisvert, L.; Goldberg, K. I. *Acc. Chem. Res.* **2012**, *45*, 899.
(3) Yin, G. *Coord. Chem. Rev.* **2010**, *254*, 1826.
(4) Rohde, J.-U.; In, J.-H.; Lim, M. H.; Brennessel, W. W.; Bukowski, M. R.; Stubna, A.; Muenck, E.; Nam, W.; Que, L., Jr. *Science* **2003**, *299*, 1037.
(5) Berry, J. F.; Bill, E.; Bothe, E.; George, S. D.; Mienert, B.; Neese, F.; Wieghardt, K. *Science* **2006**, *312*, 1937.
(6) Popescu, D.-L.; Chanda, A.; Stadler, M.; Tiago, d. O. F.; Ryabov, A. D.; Muenck, E.; Bominaar, E. L.; Collins, T. J. *Coord. Chem. Rev.* **2008**, *252*, 2050.
(7) de Oliveira, F. T.; Chanda, A.; Banerjee, D.; Shan, X.; Mondal, S.; Que, L., Jr.; Bominaar, E. L.; Muenck, E.; Collins, T. J. *Science* **2007**, *315*, 835.
(8) Anson, F. C.; Collins, T. J.; Coots, R. J.; Gipson, S. L.; Richmond, T. G. *J. Am. Chem. Soc.* **1984**, *106*, 5037.
(9) Kirksey, S. T., Jr.; Neubecker, T. A.; Margerum, D. W. *J. Am. Chem. Soc.* **1979**, *101*, 1631.
(10) Collins, T. J.; Nichols, T. R.; Uffelman, E. S. *J. Am. Chem. Soc.* **1991**, *113*, 4708.
(11) Anson, F. C.; Collins, T. J.; Richmond, T. G.; Santarsiero, B. D.; Toth, J. E.; Treco, B. G. R. T. *J. Am. Chem. Soc.* **1987**, *109*, 2974.
(12) Lu, C. C.; Weyhermuller, T.; Bill, E.; Wieghardt, K. *Inorg. Chem.* **2009**, *48*, 6055.
(13) Klaeui, W.; Eberspach, W.; Guetlich, P. *Inorg. Chem.* **1987**, *26*, 3977.
(14) Betley, T. A.; Wu, Q.; Van Voorhis, T.; Nocera, D. G. *Inorg. Chem.* **2008**, *47*, 1849.
(15) Maitra, U.; Naidu, B. S.; Govindaraj, A.; Rao, C. N. R. *Proc. Natl. Acad. Sci. U.S.A.* **2013**, *110*, 11704.
(16) Bradley, D. C.; Mehrotra, R. C.; Rothwell, I. P.; Singh, A. *Alkoxo and Aryloxo Derivatives of Metals*; Elsevier: Amsterdam, 2001.
(17) Groysman, S.; Villagran, D.; Nocera, D. G. *Inorg. Chem.* **2010**, *49*, 10759.
(18) Wolczanski, P. T. *Polyhedron* **1995**, *14*, 3335.
(19) Wolczanski, P. T. *Chem. Commun.* **2009**, 740.
(20) Koch, S. A.; Millar, M. *J. Am. Chem. Soc.* **1982**, *104*, 5255.
(21) Willis, C. J. *Coord. Chem. Rev.* **1988**, *88*, 133.
(22) Buzzeo, M. C.; Iqbal, A. H.; Long, C. M.; Millar, D.; Patel, S.; Pellow, M. A.; Saddoughi, S. A.; Smenton, A. L.; Turner, J. F. C.; Wadhawan, J. D.; Compton, R. G.; Golen, J. A.; Rheingold, A. L.; Doerrer, L. H. *Inorg. Chem.* **2004**, *43*, 7709.
(23) Childress, M. V.; Millar, D.; Alam, T. M.; Kreisel, K. A.; Yap, G. P. A.; Zakharov, L. N.; Golen, J. A.; Rheingold, A. L.; Doerrer, L. H. *Inorg. Chem.* **2006**, *45*, 3864.
(24) Zheng, B. N.; Miranda, M. O.; Di Pasquale, A. G.; Golen, J. A.; Rheingold, A. L.; Doerrer, L. H. *Inorg. Chem.* **2009**, *48*, 4274.
(25) Cantalupo, S. A.; Ferreira, H. E.; Bataineh, E.; King, A. J.; Petersen, M. V.; Wojtasiewicz, T.; DiPasquale, A. G.; Rheingold, A. L.; Doerrer, L. H. *Inorg. Chem.* **2011**, *50*, 6584.
(26) Purcell, K. F.; Kotz, J. C. *Inorganic Chemistry*; W B Saunders: Philadelphia, PA, 1977.
(27) Lum, J. S.; Tahsini, L.; Golen, J. A.; Moore, C.; Rheingold, A. L.; Doerrer, L. H. *Chem.—Eur. J.* **2013**, *19*, 6374.
(28) Hannigan, S. F.; Lum, J. S.; Bacon, J. W.; Moore, C.; Golen, J. A.; Rheingold, A. L.; Doerrer, L. H. *Organometallics* **2013**, *32*, 3429.
(29) Cantalupo, S. A.; Fiedler, S. R.; Shores, M. P.; Rheingold, A. L.; Doerrer, L. H. *Angew. Chem., Int. Ed.* **2012**, *51*, 1000.
(30) Betz, R.; Klüfers, P. *Inorg. Chem.* **2009**, *48*, 925.
(31) Mkhalid, I. A. I.; Barnard, J. H.; Marder, T. B.; Murphy, J. M.; Hartwig, J. F. *Chem. Rev.* **2010**, *110*, 890.
(32) Bull, J. A. *Angew. Chem., Int. Ed.* **2012**, *51*, 8930.
(33) Braunschweig, H.; Colling, M. *Coord. Chem. Rev.* **2001**, *223*, 1.
(34) Miyaura, N. *Bull. Chem. Soc. Jpn.* **2008**, *81*, 1535.
(35) Middleton, W. J.; Lindsey, R. V., Jr. *J. Am. Chem. Soc.* **1964**, *86*, 4948.
(36) Parris, M.; Hodges, A. E. *J. Am. Chem. Soc.* **1968**, *90*, 1909.

(37) Frye, C. L.; Salinger, R. M.; Patin, T. J. *J. Am. Chem. Soc.* **1966**, *88*, 2343.
(38) Janzen, A. F.; Rodesiler, P. F.; Willis, C. J. *Chem. Commun.* **1966**, 672.
(39) Allan, M.; Janzen, A. F.; Willis, C. J. *Can. J. Chem.* **1968**, *46*, 3671.
(40) Allan, M.; Willis, C. J. *J. Am. Chem. Soc.* **1968**, *90*, 5343.
(41) Barnhart, D. M.; Lingafelter, E. C. *Cryst. Struct. Commun.* **1982**, *11*, 733.
(42) Wurzenberger, X.; Neumann, C.; Klüfers, P. *Angew. Chem., Int. Ed.* **2013**, *52*, 5159.
(43) Hunter, R. S.; Harold, R. W. *The Measurement of Appearance*; Wiley-Interscience: Hoboken, NJ, 1987.
(44) Kubelka, P.; Munk, F. *Z. Tech. Phys.* **1931**, *12*, 593.
(45) Evans, D. F. *J. Chem. Soc.* **1959**, 2003.
(46) Sur, S. K. *J. Magn. Reson.* **1989**, *82*, 169.
(47) Briend, M.; Lamy, A.; Peltre, M.-J.; Man, P. P.; Barthomeuf, D. *Zeolites* **1993**, *13*, 201.
(48) Allen, F. H. *Acta Crystallogr., Sect. B* **2002**, *58*, 380.
(49) Yang, L.; Powell, D. R.; Houser, R. P. *Dalton Trans.* **2007**, *36*, 955.
(50) Purdy, A. P.; George, C. F.; Callahan, J. H. *Inorg. Chem.* **1991**, *30*, 2812.
(51) Purdy, A. P.; George, C. F. *CCDC-HODNOD* 1999, private communication.
(52) Hynes, R.; Payne, N. C.; Willis, C. J. *J. Chem. Soc., Chem. Commun.* **1990**, 744.
(53) Miessler, G. L.; Tarr, D. A. *Inorganic Chemistry*; Pearson Education: Upper Saddle River, NJ, 2004.
(54) Cantalupo, S. A.; Lum, J. S.; Buzzeo, M. C.; Moore, C.; Di Pasquale, A. G.; Rheingold, A. L.; Doerrer, L. H. *Dalton Trans.* **2010**, *39*, 374.
(55) Bradford, P.; Hynes, R. C.; Payne, N. C.; Willis, C. J. *J. Am. Chem. Soc.* **1990**, *112*, 2647.
(56) Plenio, H. *Chem. Rev.* **1997**, *97*, 3363.
(57) Brown, I. D.; Altermatt, D. *Acta Crystallogr., Sect. B* **1985**, *41*, 244.
(58) Purdy, A. P.; George, C. F.; Callahan, J. H. *Inorg. Chem.* **1991**, *30*, 2812.
(59) Nishino, H.; Kochi, J. K. *Inorg. Chim. Acta* **1990**, *174*, 93.
(60) Chan, D. M.-T.; Fultz, W. C.; Nugent, W. A.; Roe, D. C.; Tulip, T. H. *J. Am. Chem. Soc.* **1985**, *107*, 251.
(61) Danopoulos, A. A.; Redshaw, C.; Vaniche, A.; Wilkinson, G.; Hussain-Bates, B.; Hursthouse, M. B. *Polyhedron* **1993**, *12*, 1061.
(62) Lewis, W. B.; Alei, M.; Morgan, L. O. *J. Chem. Phys.* **1966**, *44*, 2409.
(63) Connelly, N. G.; Geiger, W. E. *Chem. Rev.* **1996**, *96*, 877.
(64) Bossu, F. P.; Margerum, D. W. *J. Am. Chem. Soc.* **1976**, *98*, 4003.
(65) Margerum, D. W. *Pure Appl. Chem.* **1983**, *55*, 23.
(66) Bossu, F. P.; Chellappa, K. L.; Margerum, D. W. *J. Am. Chem. Soc.* **1977**, *99*, 2195.
(67) Gobi, K. V.; Tokuda, K.; Ohsaka, T. *Electrochim. Acta* **1998**, *43*, 1013.
(68) de Castro, B.; Freire, C. *Inorg. Chem.* **1990**, *29*, 5113.
(69) Downard, A. J.; Hanton, L. R.; McMorran, D. A.; Paul, R. L. *Inorg. Chem.* **1993**, *32*, 6028.